Journal of Materials Chemistry C

Accepted Manuscript

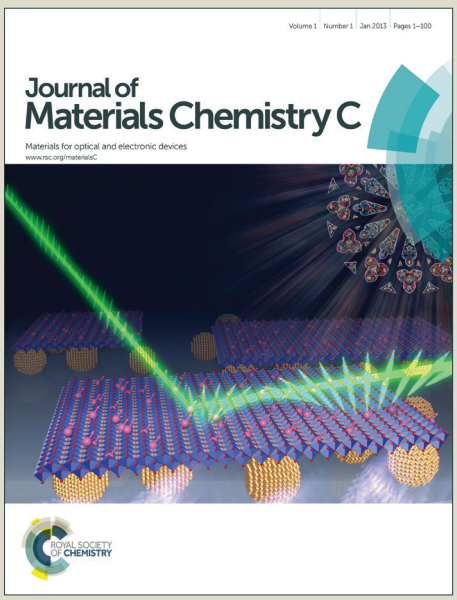

ROYAL SOCIETY OF CHEMISTRY

www.rsc.org/materialsC

Journal of Materials Chemistry C

Cite this: DOI: 10.1039/c0xx00000x

www.rsc.org/ materials

PAPER

2D-ice templated titanium oxide films as advanced conducting platforms for electrical stimulation

Hernán E. Romeo,*[a] Fernando Trabadelo,[a] Matías Jobbágy[b] and Rodrigo Parra[a]

Received (in XXX, XXX) Xth XXXXXXXXX 20XX, Accepted Xth XXXXXXXXX 20XX

DOI: 10.1039/b000000x

Directional freezing has been widely employed to prepare highly ordered three-dimensional (3D) porous assemblies. However, in this scenario, there is one concept that has not been extensively explored: by applying directional freezing to a nanoparticle (NP) dispersion supported on a substrate, two-dimensionally (2D) patterned films may be produced. In this study, tunable 2D-patterning of TiO_2-NP dispersions on alumina substrates is demonstrated. By imposing different temperature gradients throughout the ceramic dispersion coatings, both homogeneous (non-patterned) and highly aligned patterned topologies (consisting of parallel grooves) were produced. In the case of patterned films, the orientation of the grooves was modulated from those oriented along the freezing direction to those perpendicularly oriented to the temperature gradient. Thermally-induced reduction of the prepared films led to electrically conducting titanium oxide Magnéli phases. The measured resistances were strongly dependent on the orientation of the aligned patterns. To demonstrate the possibility of employing these structured films as electrical stimulation-related supports, a stimulator electronic circuit was developed and connected to the prepared films. Charge-balanced biphasic stimulus pulses with tunable current amplitudes and frequencies were successfully delivered through the conducting 2D-patterned assemblies.

1. Introduction

Nanochemistry aims at extending the traditional length scales of synthetic chemistry to specially exploit the collective properties of organized assemblies.[1] Structurally organized materials (organic, inorganic, nanocomposites) have attracted much attention for many emerging applications such as catalysis,[2] energy storage,[3] nanomedicine,[4] biotechnologies, among others. The idea in all these cases has been mainly based on offering an appropriate combination of an extended internal reactive surface, given for instance by narrow pores (micropores), with facile molecular transport through wide paths leading to and from these micropores.[5] Particularly, materials with aligned micro- and macrostructures are of interest for a wide range of applications such as microfluidics,[6] molecular filtration,[7] electronics,[8] tissue engineering,[9] among others. Likewise, synthetic aligned porous structures may be also used to mimic natural structured materials such as bone and nacre.[10]

Demands for these advanced materials, able of being applied in new and emerging technologies, have triggered the development of different structuring techniques. Compared to dry processing routes, wet shaping processes are able of leading to materials with complex shapes, being effective at the same time to obtain both dense and porous materials. Among the different wet structuring processes, cost-effective freezing techniques (involving solutions, colloidal dispersions) have been developed and explored as unique routes to produce highly organized porous materials,[11] though freeze casting has also been applied to produce dense monoliths.[12,13] The freezing technique involves three stages: (i) actual freezing, (ii) primary drying, and (iii) secondary drying.[14] The freezing stage is accomplished by contacting a liquid sample with or placing it in a cold bath. This leads to the solidification of the solvent medium which finally determines the resulting microstructure and volume change associated to the phase transformation. In this respect, there is no doubt that water-based systems have been the most investigated ones. During the freezing step, most solutes are segregated from the ice phase, giving rise to a hierarchical assembly characterized by "fences" of matter enclosing ice.[15] The final removal of ice *via* freeze drying (primary drying stage) allows obtaining macroporous materials, generated from the voids left by the initially formed ice. This step is usually the most time-consuming, which is directly related to the ice sublimation rate and it is determined by factors such as the vacuum level, shelf temperature, sample volume and exposed surface area.[16] Secondary drying is related to strongly adsorbed solvent, reason why lower vacuum levels (compared to primary drying) are generally needed. During the freezing stage different conditions, including freezing temperature, solute concentration, solvent type, presence of additives and direction of freezing, can have (and do have) a great impact on the resulting structure.[17] As to the freezing direction, it has been recognized to exert one of the major effects on the final morphology.[18] When the temperature distribution is uniform throughout the sample, anisotropic ice crystal growth is hindered and homogeneous microstructures are obtained. However, by applying a high temperature gradient across the sample (which is termed *directional freezing*) anisotropic ice crystal growth along the freezing direction is favored. This occurs due to the chemical potential difference among the different ice crystal facets.[19] The final removal of oriented ice generates materials with highly aligned unidirectional macropores.[20]

The fundamental principles of directional freezing are very well established and documented in excellent reviews.[17,19,21] As already mentioned, the formation of porous micro-/

macrostructures relies on the rejection of particles (and/or solutes initially dissolved) by the advancing solidification front and the subsequent concentration of them between the ice lamellae. However, this only happens if the breakdown of the solidification front to a non-planar morphology takes place. When the solidification velocity is extremely low, lamellar (and consequently porous) microstructures may dissapear. This is because the ice front velocity, dictated by the temperature gradient, is much lower than the critical particle entrapment velocity. This leads to a stable planar advancing ice front, in which case all of the particles and/or solutes are rejected together and directional microstructures along the freezing direction cannot be produced. While all of these aspects have been taken into consideration to prepare materials with complex anisotropic porous microstructures, such as lamellar, dendritic, parallel, columnar and aligned porous scaffolds,[22-24] these studies have only dealt with three-dimensional (3D) arrangements.

In this scenario, there is one concept that has not been extensively explored yet: by applying directional freezing to a nanoparticle (NP) dispersion supported on a substrate, it would be possible to generate two-dimensionally (2D) patterned films. While it is true that studies on films and membranes prepared by freeze-tape-casting processes have already been published,[25,26] in these cases only through-thickness porosity has been developed. Only one study on the directional freezing of gold NP dispersions on mica surfaces (obtaining oriented metallic patterns) has been reported.[27] However, systematic evaluation of the possibility of modulating the gold patterns has not been performed. The possibility of controlling both the generation of homogeneous or anisotropic structures and the degree of segregation of NPs by imposing different temperature gradients would allow us to modulate the 2D-pattern obtained.

In this study, titanium dioxide NP (TiO_2-NP) aqueous dispersions were induced to self-organize on alumina (Al_2O_3) substrates during the course of a directional freezing process. Both homogeneous (non-patterned) and highly oriented TiO_2 films were successfully prepared by controlling the freezing conditions. In the case of patterned films (consisting of parallel grooves), the orientation of the grooves was modulated from those oriented along the freezing direction to those perpendicularly oriented with respect to the freezing direction. A possible mechanism for the self-organization and tunable orientation was proposed. Finally, structurally-aligned TiO_2 films were thermally treated in a reducing atmosphere (H_2/Ar) in order to generate oxygen vacancies in the TiO_2 (rutile) structure. This thermally-induced reduction led to mixtures of electrically conducting substoichiometric titanium oxide phases (known as Magnéli phases) which allowed to introduce a new functional property (electrical conductivity) to the structured films. To demonstrate the effect of the orientation of the aligned conductive patterns on the electrical properties, electrical resistances of the films (parallel to and perpendicular to the freezing direction) were determined. The measured resistances were strongly dependent on the orientation of the aligned patterns.

Because of the known electrical,[28] antiinflamatory[29] and biocompatibility[30] properties of the Magnéli phases, in combination with the presence of freezing-induced aligned grooves on the prepared films, these 2D assemblies may find applications on biomedical-related areas. As to this purpose, the possibility of employing the prepared structured films as electrical stimulation-related supports was evaluated. To this end, a stimulator electronic circuit was developed. Charge-balanced biphasic stimulus pulses (with tunable current amplitudes and frequencies) were successfully delivered through the conducting 2D-patterned structures.

To the best of our knowledge, this is the first report on the simultaneous combination of directional freezing and electrically conducting titanium oxide phases to render orientation-dependent electrically active 2D-patterned assemblies, able of being employed as platforms on tunable electrical stimulation applications.

2. Experimental

2.1. Preparation of TiO_2 dispersions.

Fig. 1 shows a TEM image of the Degussa P25 TiO_2-NPs used for preparing the aqueous dispersions used in this work. The powder was composed of particles of average diameter 20-30 nm. For preparing dispersions, 9.3 g of polyvinylpyrrolidone (PVP, Aldrich, ~1.3MDa) were dissolved in 150 mL of distilled water. Then, 31.5 g of TiO_2 were added to the resulting solution and dispersed by means of a T25 Ultra-Turrax instrument at 25000 rpm. TiO_2-NP dispersions exhibited long time stability (over 24 h) which represented a suitable time for preparing and processing samples, with no sedimentation nor precipitation occurring during this period.

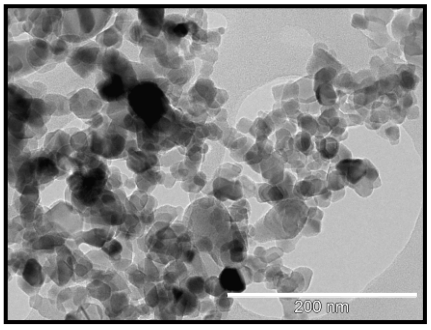

Fig. 1 TEM image of TiO_2 nanoparticles used. Bar: 200 nm.

2.2. Preparation of alumina-supported TiO_2 films.

Before film deposition, alumina substrates (2.5 cm x 1 cm) were washed with aqueous detergent solution followed by ethyl alcohol and acetone, and finally heated for drying. The prepared TiO_2-NP dispersions were used for the deposition of films on clean substrates by a squeegee technique, using adhesive Scotch-tape to control the thickness of the coatings.[31,32] Dispersions thus deposited did not drain out from the substrates during vertical dipping due mainly to the high viscosity of the prepared slurries (tests performed previously to evaluate this condition demonstrated that hours are in fact needed for the deposited dispersions to flow down with gravity). Films were subsequently stored in a 100% relative humidity incubator at room temperature in order to avoid solvent evaporation, and kept under this condition until they were directionally frozen.

2.3. Directional freezing of alumina-supported TiO_2 films.

The prepared TiO_2-NP films were vertically dipped at variable advancing ice front rates into a liquid nitrogen bath maintained at 77 K and under room pressure (Fig. 2).

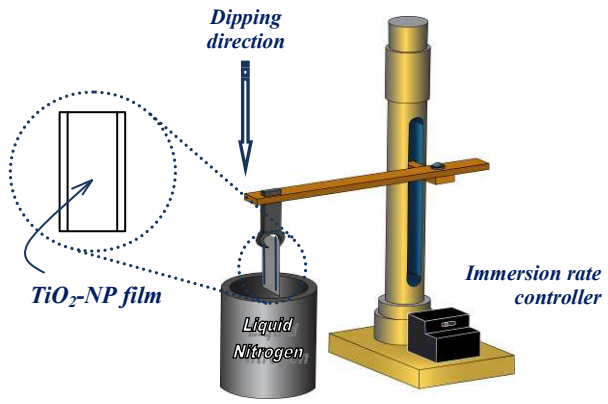

Fig. 2 Schematic representation of the directional freezing process.

Surface 2D-patterning was modulated by the temperature gradient imposed to the samples. This was carefully controlled with the immersion rate at which samples were induced to freeze. Four conditions were evaluated: (1) films submitted to high freezing rates (30 mm/min), (2) films submitted to intermediate freezing rates (15 mm/min), (3) films immersed at low rates (5 mm/min), and (4) films exposed to cold nitrogen vapours (samples did not contact the liquid phase, and were frozen at the lowest rate: ~ 1 mm/min). Once the films start freezing, the imposed temperature gradient keeps the growing ice into a steady state at a self-controlled and reproducible rate which finally governs the whole directional freezing process.

Finally, the unidirectionally frozen samples were freeze-dried for 48 h (100 mtorr and - 45 ºC) using a VirTis Benchtop SLC (2KBTES-SS) freeze-drier.

2.4. Thermal treatments on freeze-dried films.

The lyophilized films were heat-treated at 1000 ºC for 1.5 h, with heating and cooling rates of 5 ºC/min, for sintering in an air atmosphere. For this purpose, an electric high-temperature furnace (Carbolite RHF 17/6S) was used.

Electrically conducting films were obtained after a high-temperature reducing process. Sintered films were treated at 1000 ºC for 3 h under H_2/Ar (5% H_2) atmosphere in order to obtain Ti sub-oxide phases. Both sintered and reduced films were finally characterized.

2.5. Experimental design for biphasic electrical stimulation.

The stimulator electronic circuit used as an excitation source was composed of two sub-systems: (1) an embedded control board (ECB) responsible for handling the user interface and generating the two pulse-width modulation (PWM) signals, and (2) an analog circuit assembly (ACA) responsible for signal adaptation and control (Scheme 1).

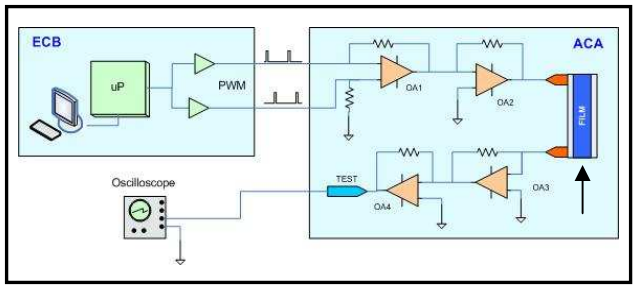

Scheme 1 Schematic representation of the electronic circuit used to output the biphasic stimulation pulses.

Stimulating PWM outputs were easily configured by means of a keyboard and an LCD display. PWM signals were adjusted in frequency, amplitude and duty cycle. The programmed signals then fed the output stage of the analog circuit for final biphasic current pulse adaptation by means of four operational amplifiers (OA 1, 2, 3 and 4 in Scheme 1). The output frequency was set within the 1 Hz to 1 kHz range, and current amplitudes were modulated from 5 to 50 μA. Films under test were placed on two copper paths as electrical contacts (indicated by a black arrow in Scheme 1). In order to measure the circulating current along the conducting films, an analog operational circuit was employed as a current to voltage converter. Finally, the output voltage was tested with a Tektronix TDS2024C oscilloscope. All stimulations were performed at room temperature.

2.6. Characterization techniques.

The morphology and size distribution of commercial TiO_2 NPs were assessed by means of transmission electron microscopy (TEM) in a Philips CM200 microscope.

Film surface morphologies were investigated by scanning electron microscopy (SEM) on metalized samples by means of a Jeol JXA-8600 instrument.

Grazing incident X-ray diffraction (GI-XRD) patterns of the prepared films were recorded with an X'Pert Pro PANalytical difractometer, employing the Cu K_α line (wavelength 1.5406 Å). The electrical voltage and current were 40 kV and 30 mA, respectively. Data were collected for 2θ angles ranging between 10º and 80º with a step size of 0.02º 2θ and 0.5s acquisition time per step.

Film topographical features (grooves depth) were determined with a KLA Tencor Alpha Step D100 profilometer, at a scan rate of 0.03 mm/s.

The resistance of the conducting films was calculated from the slope of current-voltage plots. Measurements were carried out at room temperature, both along and perpendicularly to the freezing direction, by means of a Xantrex XFR 300-4 DC power supply unit and a HP 34401A multimeter, with a distance of 0.8 cm between test leads.

3. Results and discussion

Fig. 3 shows a photograph and SEM images of a sintered TiO_2 film prepared from the highest freezing rate (30 mm/min). From now on, this sample will be referenced as *30-TiO_2* film.

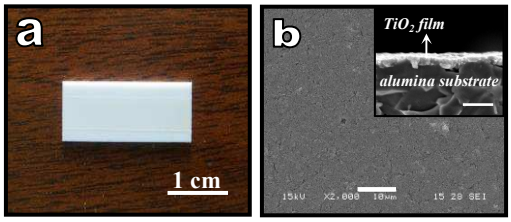

Fig. 3 Photograph (a) and SEM images (b) corresponding to 30-TiO_2 film sintered at 1000 ºC for 1.5 h. Scale bars in (b): 10 µm.

Homogeneous ~ 2-3 µm thick films (Fig. 3b inset) were obtained on alumina substrates, which retained their structural stability after sintering. According to the high freezing rate employed, non-patterned surfaces were obtained (see also Fig. S1, Supplementary Information). This is expected when high ice formation velocities are induced. A high rate of immersion into liquid nitrogen prevents generating a high temperature gradient throughout the sample, which leads to isotropic ice growth and consequently to homogeneous microstructures. Structures like the one shown in Fig. 3b (and Fig. S1 in Supplementary Information) are consistent with high particle expulsion hindrance and randomly oriented ice crystal growth. Similar results were obtained for the 30-TiO_2 film before sintering. This corroborated that the thermal treatment did not disrupt the initial non-patterned homogeneous structure.

Fig. 4 shows the GI-XRD pattern corresponding to the 30-TiO_2 film heat-treated at 1000 ºC. The diffraction pattern corresponds to a single phase which was indexed to the rutile phase of TiO_2, in agreement with the JCPDS 76-0649 file. The same pattern was registered for every film treated at 1000 ºC, regardless of the immersion rate applied during the directional freezing stage.

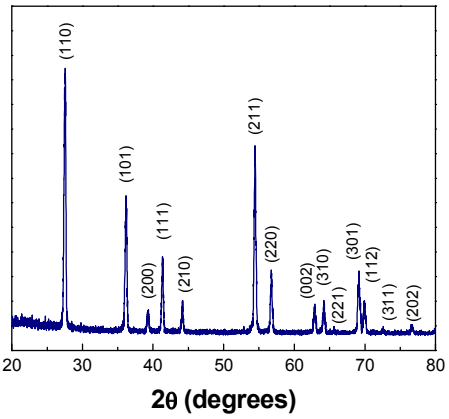

Fig. 4 GI-XRD pattern of 30-TiO_2 film sintered at 1000 ºC; *hkl* indexing corresponds to rutile main reflexions.

In order to assess the possibility of modulating the film surface topology, different immersion rates were then evaluated. Taking the 30 mm/min as the velocity from which homogeneous and non-structured films are obtained (30-TiO_2 sample), lower advancing ice front rates were then tried. This would in principle allow entering the velocity gap where disruption of the planar advancing ice front takes place, leading to Mullins-Sekerka instability and consequently to anisotropic ice growth.[33,34] The evaluation of the modulated 2D-patterning according to the freezing conditons will be analized in what follows.

Fig. 5 shows SEM images, captured under different magnifications, of a TiO_2 film immersed into liquid nitrogen at a lower rate (15 mm/min) compared to that of the 30-TiO_2 sample. This sample will be referred to as *15-TiO_2* film.

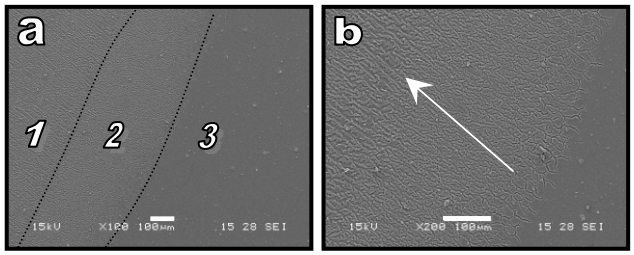

Fig. 5 SEM images corresponding to 15-TiO_2 film sintered at 1000 ºC for 1.5 h. Image (b) corresponds to a magnification of (a). *1*, *2* and *3* in (a) depict regions where aligned, transitional and non-ordered topologies were respectively identified (Dotted lines are eye-guides). Arrow shows the freezing direction. Bars: 100 µm.

Experimental evidence showed that it is effectively possible to induce the 2D breakdown of the solidification front to a non-planar advancing ice morphology, by simply modifying the directional immersion rate. This effect has been already reported for 3D porous structures,[23] however, to the best of our knowledge, this is the first time that this morphological transition is evidenced on patterned films. Region 1 depicted on Fig. 5a corresponds to the furthest end of the TiO_2 film with respect to the cooling liquid surface. This region is composed of highly aligned grooves along the freezing direction and it is preceded by a transitional region (region 2, neither ordered nor disordered) which links to a homogeneous non-oriented topology (region 3) (see details in Fig. S2, Supplementary Information).

By further lowering the immersion rate into liquid nitrogen (which is, by increasing the temperature gradient throughout the sample), the degree of order was extended to the whole film surface. This was accomplished on a film immersed at 5 mm/min. This sample will be referred to as *5-TiO_2* film. Fig. 6 shows SEM micrographs corresponding to a sintered 5-TiO_2 film (see microstructure details in Fig. S3, Supplementary Information).

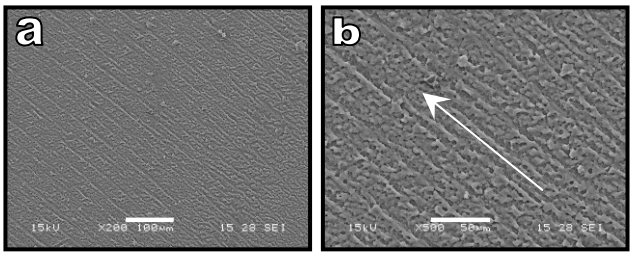

Fig. 6 SEM images corresponding to 5-TiO_2 film sintered at 1000 °C for 1.5 h. The arrow shows the freezing direction. Bars: 100 µm (a), and 50 µm (b).

Sample 5-TiO_2 exhibited highly oriented parallel patterns extending throughout the whole surface, with grooves ~ 5 µm wide and ~ 1.5 µm depth, as measured by profilometry.

A detail of groove morphology is presented in Fig. 7.

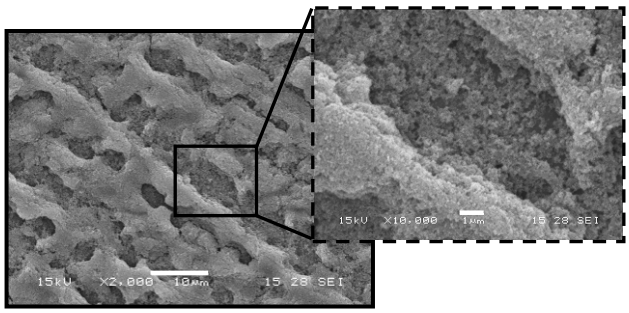

Fig. 7 Detail of grooves developed in sintered 5-TiO_2 film. Bar: 10 µm (1 µm on the inset).

A ´fish-bone` morphology was obtained, as is also commonly reported for 3D-assemblies processed by directional freezing.[11,27] This results from the side branches that form when TiO_2 NPs freeze-concentrate around the primary ice cells, which produces secondary instabilities perpendicularly oriented to the freezing direction. This finally leads to the bridging of primary TiO_2 paths (aligned along the freezing direction) by shorter ceramic NP partitions (perpendicularly oriented to the freezing gradient). The surface seen between ridges is composed of TiO_2 nanoparticles (although a ´naked` alumina surface may be also identified) but less interconnected compared to the joining bridges. A closer inspection of the surface is shown Fig. S4 in the Supplementary Information.

After employing the lowest dipping rate attainable with the immersion device (5 mm/min), an attempt to further lower the freezing rate was made. This would allow, *a priori*, to take control over the relative dominance of ice nucleation rate and crystal growth. For this purpose, the cold vapours of the freezing liquid were used. This was accomplished by submitting a TiO_2 film to nitrogen vapour, not placing the sample in contact with the liquid nitrogen. The film was kept at a distance of 3 cm from the liquid surface and it remained at that distance until it was completely frozen.

It has been widely reported that very slow freezing rates on aqueous dispersions lead to the rejection of particles by the planar advancing ice front. Thermodinamically, the interfacial free energy between the particles and the solidifying front (σ_{sp}) should be larger than the sum of interfacial free energies associated with solid-liquid (σ_{sl}) and particle-liquid (σ_{pl}) interactions for the particles to be effectively rejected forward as the planar ice advances ($\sigma_{sp} > \sigma_{sl} + \sigma_{pl}$).[35] This effect has been succesfully employed to collect particles on one side of the studied system once solidification was achieved, representing a useful method for removing pollutants (water purification).[36] In addition to the thermodynamic criterion, the rejection of NPs will depend on extra forces exerted on them. For particles close to the solidification front, the most important forces are repulsive and drag ones.[35] The relationship between these forces can in fact reinforce the thermodynamic contribution. Taking these concepts into consideration, only dragging of the TiO_2 NPs would be expected from a very low freezing rate imposed to the films, and non-patterned morphologies would have to be predicted. However, it has been already demonstrated that NPs can only be concentrated by the advancing ice front up to a certain breakthrough point.[37] The TiO_2 NPs may be pushed along the solid-liquid interface until the capillary drag force is counterbalanced by the force resulting from the osmotic pressure of the suspension.[23] If this happens, patterned films (but in this case, perpendicularly oriented to the freezing direction) might be produced. This is, in fact, demonstrated herein.

Fig. 8 depicts SEM images of the film produced after the freezing process into nitrogen vapour. The freezing rate (~ 1 mm/min) was measured from the advancing solidification front seen on the substrate being frozen (the dispersion/ice interface was clearly visualized as a horizontal opaque layer advancing upwards). This film will be referenced as *1-TiO_2* sample.

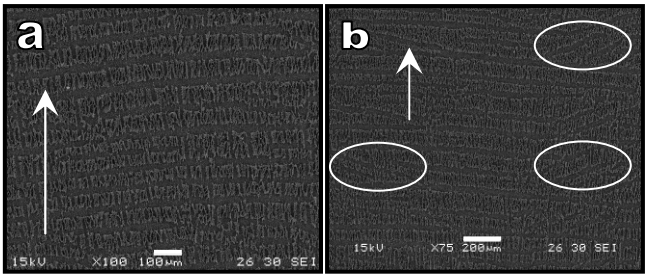

Fig. 8 SEM images of the surface developed in sintered 1-TiO_2 film. Arrows indicate the freezing direction. Bars: 100 µm (a) and 200 µm (b).

Highly-aligned TiO_2 patterns perpendicularly oriented to the freezing direction were obtained. The morphologies seemed to be similar to those obtained from the so-called "ice lenses" which have been already reported for other ice templated colloidal dispersions.[38,39] A 90-degree tilting change (compared to 5-TiO_2 sample) was produced by simply exposing the film to liquid nitrogen vapour (Fig. 8a) (See details in Fig. S5a, Supplementary Information). This behaviour may be explained by a continuous sequence of dragging and ´engulfing` events, both temporally and spatially interspersed. The growing planar ice front would reject the NPs as it advances on the alumina substrate, engulfing them when the osmotic pressure of the deposited suspension equals the dragging force. However, tilted grooves (at about 45º with respect to the freezing direction) were also observed in the same sample (Fig. 8b, indicated by ellipses) (See also details in Fig. S5b, Supplementary Information). This effect may be associated with a change of temperature gradient orientation during the freezing process, as a consequence of the freezing conditions (the nitrogen atmosphere has to be precisely controlled). The tilted features closely depend on the relationship between the crystal growth rate along the preferred crystal growth direction and the rate along the temperature gradient direction.[17] Changes in direction of the temperature gradient due to vapour fluctuations could have induced, in this case, orientational changes during TiO_2 NP rejection. Although this structured film was generated from a phenomenon which is mechanistically different from that previously discussed for the other films, highly ordered TiO_2 paths separated by grooves ~ 20-30 µm wide were also obtained.

The presence (in 5-TiO_2 and 1-TiO_2 films) or absence (in 30-TiO_2 film) of 2D patterns could produce a significant influence on transport properties associated with the film anisotropic features, and this is precisely one of the most interesting aspects that can be exploited from these 2D structures.

Directionally frozen 3D porous scaffolds developed from TiO_2 NP dispersions have been demonstrated to be excellent supporting materials. The presence of aligned ´highways` throughout the whole scaffolds has been shown to be useful not only to the transport of analytes through the as-developed macroporosity, but of incident radiation as well (orientation-dependent light harvesting devices).[40] Likewise, both powdered and bulky TiO_2 materials have been used as precursors to obtain electrically conductive phases.[41] This is possible because of the existence of substoichiometric compositions, ranging from TiO_2 to Ti_2O_3, in the titanium-oxygen phase diagram.[28,42] These intermediate phases (*Magnéli* phases) form a homologous series Ti_nO_{2n-1}, with $4 \leq n \leq 10$. When moving from TiO_2 to Ti_2O_3 the *d* band occupation across the series increases, and the electronic structure of the material consequently changes. This change in electronic structure is in fact responsible for the high electrical conductivity displayed by titanium oxide Magnéli phases.[42,43] Depending on the synthesis conditions, Magnéli suboxides can exhibit a wide range of electrical conductivities. They are synthesized from rutile TiO_2, by typically heating the sample to temperatures of about 1000-1050 ºC in a reducing atmosphere. In addition to the electrical conductivity related to these phases, the biocompatibility and chemical stability associated with these titanium oxides have made these ceramic phases to be extensively investigated in both electrochemical[44] and biomedical-related areas.[30]

In this study, to demonstrate both the degree of organization achieved in the anisotropically patterned films and the effect of pattern orientation on electrical conduction properties, sintered samples were then thermally treated in a reducing atmosphere to generate Magnéli phases. Electrical resistances of the Magnéli films (parallel to and perpendicular to the freezing direction) were determined. Fig. 9 shows a photograph and the corresponding GI-XRD pattern of the reduced 5-TiO_2 film.

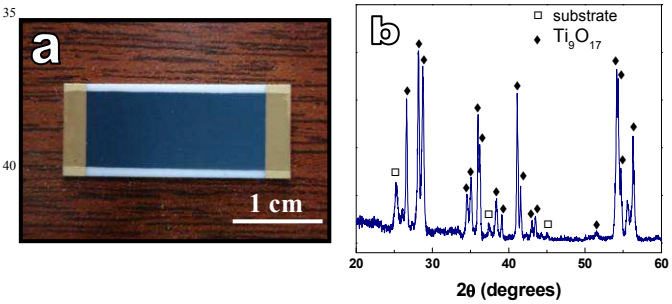

Fig. 9 Photograph (a) and GI-XRD (b) corresponding to 5-TiO_2 film reduced at 1000 ºC for 3 h in a H_2/Ar atmosphere. Film in (a) exhibits Au electrodes deposited perpendicularly to the freezing direction.

Optically homogeneous films were obtained after the reducing protocol. Blue/black ceramic surfaces are indicative of the generation of oxygen vacancies, which allows explaining the film color change on the basis of color center generation.[45] The film surface features were not modified by the high-temperature reducing process, as revealed by SEM (Fig. S6 in Supplementary Information). Fig. 9b shows the diffraction pattern associated with a mixture of Magnéli phases. Indexing revealed the presence of Ti_9O_{17} (JCPDS 00-50-0791) as the main phase, although traces of Ti_6O_{11} (JCPDS 10-85-1058) and Ti_7O_{13} (JCPDS 00-50-0789) might also be present, in good agreement with the review article by Szot *et al.*[46] Analogous results were obtained for all of the treated films, however, significant differences in electrical resistances were evidenced depending on both structuring features and pattern orientation.

The homogeneous non-patterned 30-TiO_2 film exhibited the lowest resistance values (3-4 kΩ) compared to its freeze-patterned counterparts (5-TiO_2 and 1-TiO_2 samples) (see Table 1).

Table 1 Characteristics and electrical resistances of the prepared films

Sample	*Freezing Rate (mm/min)*	*Patterning*	*Resistance Dependent on Surface Orientation*	*Electrical Resistance*	
				Along f. d.	Perpendicular to f. d.
30-TiO_2	30	absent	no	3-4 kΩ	3-4 kΩ
5-TiO_2	5	along the f. d.	yes	3-4 kΩ	10 kΩ
1-TiO_2	1	perpendicular to the f. d.	yes	open circuit	30-40 MΩ

f. d.: *freezing direction*

The resistance of 30-TiO_2 sample did not show any dependence on surface orientation, as expected from non-patterned conducting surfaces due to the isotropic and continuous network of interconnected grains. As to the freezing-patterned films, they interestingly evidenced strong orientation-dependent electrical resistences. Higher resistance values, compared to 30-TiO_2 sample, were explained on the presence of grooves taking part of the film topology. For the 5-TiO_2 film, measurements determined along the freezing direction gave values of 3-4 kΩ (the same as that for the non-patterned sample), while it displayed a resistance of ~ 10 kΩ perpendicularly measured to the structured patterns. On the other hand, for the 1-TiO_2 film, measurements determined along the freezing direction (perpendicularly to the ordered fringes) gave an open circuit response, which was attributed to the poor film continuity as revealed by SEM (Fig. 8, and Fig. S4 in Supplementary Information). Measurements performed perpendicularly to the freezing direction (along the aligned conductive paths) gave resistance values of 30-40 MΩ. Such high values were assigned to the partial contact among titanium oxide particles along conducting strips (Fig. 8, and Fig. S4 in Supplementary Information). The experimental results demonstrated that, in fact, the anisotropic features effectively exert a strong influence on electrical transport properties of the 2D-ice templated films. As a consequence, the possibility of employing these conducting assemblies as electrical stimulation-related supports was evaluated.

Electrical stimulation (ES) has been shown to be a promising technique for a variety of stimulation-assisted medical treatments. Electric pulses have been employed to induce responses in nerve, skin and skeletal tissues.[47,48] In particular, it is known that ES affects neuronal activity by triggering a change of voltage gradient through neuronal membranes,[49] reason why this approach has recently raised much interest as a potential therapeutic tool for the treatment of injuries related to the peripheral nervous system (PNS).[50] As to this application,

whether monophasic or biphasic current pulses is better for peripheral nerve regeneration is still an issue of debate. While it is true that monophasic stimuli can lead to the orientation of cell membrane proteins creating in this way an "electrical cue" for regeneration,[51,52] it is widely accepted that biphasic stimulation has several advantages over the monophasic approach. Among these advantages, biocompatibility, charge balance and maintenance of a constant pH are the most remarkable ones. In addition to all of these electrical stimulation-related aspects, it has been also demonstrated that "guidance cues" (given by topographycally-structured surfaces made up of parallel grooves) provide considerable *in vitro* neurite guidance information.[53] In the same line of research, Rajnicek and McCaig investigated the mechanism by which contact guidance, given by grooved surfaces, affected the pattern of growth cones of both embryonic *Xenopus* spinal neurites and rat hippocampal neurites.[54] In summary, not only electrical stimulation but topographical features as well have been demonstrated to exert strong morphogenetic stimuli for developing neurons, with all of these characteristics being very well stated in a recent review.[55] All this knowledge could in principle be thought to have a strong impact on *in vitro* stimulating approaches towards a better understanding of the mechanisms involved on neuronal evolution.

For all of this, and envisioning a potential use of the prepared films as *in vitro* electrical-test supports, a stimulator electronic circuit was developed and connected to the patterned films. Fig. 10 shows photographs of the two modules (ECB and ACA, see Scheme 1) that take part of the stimulating electronic circuit, and a capture of the biphasic signal obtained by testing the 5-TiO_2 film.

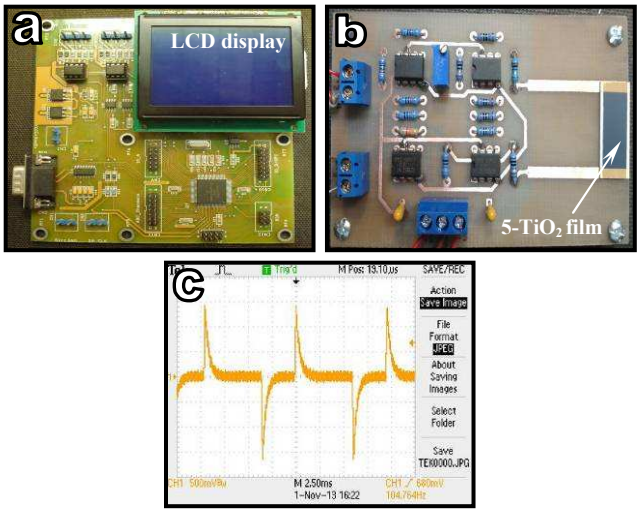

Fig. 10 (a) Embedded control board (ECB) used in to test the films, (b) analog part of the signal stimulator (ACA), and (c) oscilloscope capture of the biphasic stimulus pulses delivered through the 5-TiO_2 film.

The film was connected to the analog circuit *via* gold electrodes deposited (by sputtering) at both film ends (Fig. 10b). The applied stimulation allowed delivering electrical currents of different amplitudes and charge-balanced biphasic pulses of different frequencies. Current values from 5 to 50 μA and stimulus signals from 1 Hz to 1 kHz were succesfully delivered through the film.

The 30-TiO_2 film was employed as control sample, which gave the same electrical response as that of 5-TiO_2 specimen. The only difference between these samples is the topographical features. Sample 5-TiO_2 combines the two specific ideas of this work, namely the electrical stimulation and the oriented patterned topology.

The results shown here (taking specially into account the current and frequency ranges that can be scanned, and the biocompatibility properties recognized to Magnéli phases) give support to the potential use of these electrically conducting structured platforms on *in vitro* cell-related stimulation therapies.

4. Conclusions

Two-dimensionally patterned TiO_2 films were successfully prepared by directional freezing of TiO_2 NP aqueous dispersions deposited on alumina substrates. By carefully selecting the adequate freezing rate, it was possible to modulate the surface morphological features. On going from higher (30 mm/min) to lower (1 mm/min) freezing rates, the following sequence of 2D-assembled films was produced: non-patterned (homogeneous) films → patterned films with grooves highly aligned along the freezing direction → patterned films with grooves perpendicularly oriented to the freezing direction.

Electrically conducting films were obtained by treating sintered samples at high temperature in a reducing atmosphere. The morphological features (presence or absence of oriented 2D patterns) produced a strong influence on the electrical properties. While homogeneous films exhibited the lowest resistances and showed no dependence on measurement orientation, highly-oriented grooved films evidenced significant orientation-dependent electrical resistance values. In order to evaluate the possibility of using these patterned systems as *in vitro* electrical stimulation-related supports, a stimulator electronic circuit was developed and connected to the prepared films. Charge-balanced biphasic stimulus pulses, with tunable current amplitudes and frequencies, were successfully delivered through the 2D assemblies. This gave support to the potential use of the combined approach (stimulating circuit + patterned conducting films) on *in vitro*-assisted medical studies. Work is in progress in this direction.

The proposed method towards tunable 2D-patterned films exhibits the following interesting features: (i) cost-effective facilities are required, (ii) NPs of different nature (metallic, semiconducting, polymeric) could be *a priori* employed, provided their dispersions are stable, (iii) the procedure can be scaled up on substrates of several centimeters, and (iv) the proposed idea could be implemented on different water-soluble/dispersable polymeric-NP combinations, leading to novel multifunctional composite films. All these features could be used to prepare new materials displaying a wide range of properties made to order.

Acknowledgements

This work was supported by the National Research Council (CONICET, Argentina), the National Agency for the Promotion of Science and Technology (ANPCyT, Argentina), the University of Mar del Plata and the University of Buenos Aires (Argentina).

Authors specially thank Víctor N. Romeo for the construction of the controlled-immersion device. Thanks are due to Humar Ávila Vanegas for Fig. 2.

Electronic Supplementary Information

Surface topographical details by SEM characterization are available.

Notes and references

[a] *Instituto de Investigaciones en Ciencia y Tecnología de Materiales (INTEMA), Universidad Nacional de Mar del Plata, Consejo Nacional de Investigaciones Científicas y Técnicas (CONICET), 7600, Mar del Plata, Argentina; E-mail: hromeo@fi.mdp.edu.ar*
[b] *Instituto de Química Física de los Materiales, Medio Ambiente y Energía (INQUIMAE), Universidad de Buenos Aires, Consejo Nacional de Investigaciones Científicas y Técnicas (CONICET), C1428EHA, Buenos Aires, Argentina.*

1. G. A. Ozin and A. C. Arsenault, *Nanochemistry: a chemical approach to nanomaterials*. RSC Publishing, Cambridge, United Kingdom (**2005**).
2. M. Choi, H. S. Cho, R. Srivastava, C. Venkatesan, D. H. Choi and R. Ryoo, *Nat. Mater.*, 2006, **5**, 718.
3. L. Nyholm, G. Nyström, A. Mihranyan, M. Stromme, *Adv. Mater.*, 2011, **23**, 3751.
4. M. Vallet-Regí, *J. Intern. Med.*, 2009, **267**, 22.
5. B. L. Su, C. Sanchez, X. Y. Yang, *Hierarchically structured porous materials: from nanoscience to catalysis, separation, optics, energy, and life science*. Wiley-VCH, Weinheim, Germany (**2012**).
6. S. R. Quake and A. Scherer, *Science*, 2000, **290**, 1536.
7. A. Yamaguchi, F. Uejo, T. Yoda, T. Uchida, Y. Tanamura, T. Yamashita and N. Teramae, *Nat. Mater.*, 2004, **3**, 337.
8. H. Gu, R. Zheng, X. Zhang and B. Xu, *Adv. Mater.*, 2004, **16**, 1356.
9. C. Y. Xu, R. Inai, M. Kotaki and S. Ramakrishna, *Biomaterials*, 2004, **25**, 877.
10. S. Deville, E. Saiz, K. Ravi, R. V. Nalla and A. P. Tomsia, *Science*, 2006**, 311**, 515.
11. H. E. Romeo, C. E. Hoppe, M. A. López-Quintela, R. J. J. Williams, Y. Minaberry and M. Jobbágy, *J. Mater. Chem.*, 2012, **22**, 9195.
12. O. A. Shlyakhtin, Y. J. Oh and Y. D. Tretyakov, *J. Eur. Ceram. Soc.*, 2000, **20**, 2047.
13. K. Kuribayashi and P. S. Nicholson, *Mater. Res. Bull.*, 1980, **15**, 1595.
14. C. Chen and W. Wang, *Dry Technol.*, 2007, **25**, 29.
15. M. C. Gutiérrez, Z. Y. García-Carbajal, M. Jobbágy, F. Rubio, L. Yuste, F. Rojo, M. L. Ferrer and F. del Monte, *Adv. Funct. Mater.*, 2007, **17**, 3505.
16. X. Tang and M. J. Pikal, *Pharm. Res.*, 2004, **21**, 191.
17. W. L. Li, K. Lu and J. Y. Walz. *Int. Mater. Rev.*, 2012, **57**, 37.
18. H. Zhang and A. L. Cooper, *Adv. Mater.*, 2007, **19**, 1529.
19. S. Deville, *Adv. Eng. Mater.*, 2008, **10**, 155.
20. M. C. Gutiérrez, M. L. Ferrer and F. del Monte, *Chem. Mater.*, 2008, **20**, 634.
21. L. Qian and H. Zhang, *J. Chem. Technol. Biotechnol.*, 2011, **86**, 172.
22. J. C. Han, L. Y. Hu, Y. M. Zhang and Y. F. Zhou, *J. Am. Ceram. Soc.*, 2009, **92**, 2165.
23. S. Deville, E. Maire, A. Lasalle, A. Bogner, C. Gauthier, J. Leloup and C. Guizard, *J. Am. Ceram. Soc.*, 2009, **92**, 2489.
24. E. Landi, F. Valentini and A. Tampieri, *Acta Biomater.*, 2008, **4**, 1620.
25. L. Ren, Y-P. Zeng and D. Jiang, *J. Am. Ceram. Soc.*, 2007, **90**, 3001.
26. M. K. Lee, N-O. Chung and J. Lee, *Polymer*, 2010, **51**, 6258.
27. H. Zhang, I. Hussain, M. Brust, M. F. Butler, S. P. Rannard and A. I. Cooper, *Nat. Mater.*, 2005, **4**, 787.
28. C. Yao, F. Li, X. Li and D. Xia, *J. Mater. Chem.*, 2012, **22**, 16560.
29. R. Contreras, H. Sahlin and J. A. Frangos, *J. Biomed. Mater. Res. A*, 2007, **80A**, 480.
30. M. Canillas, E. Chinarro, M. Carballo-Vila, J. R. Jurado and B. Moreno, *J. Mater. Chem. B*, 2013, **1**, 6459.
31. C. J. Barbé, F. Arendse, P. Comte, M. Jirousek, F. Lenzmann, V. Shklover and M.Grätzel, *J. Am. Ceram. Soc.*, 1997, **80**, 3157.
32. G.P. Smestad and M. Grätzel, *J. Chem. Educ.*, 1998, **75**, 752.
33. M. F. Butler, *Cryst. Growth Des.*, 2002, **2**, 59.
34. S. Deville, E. Maire, G. Bernard-Granger, A. Lasalle, A. Bogner, C. Gauthier, J. Leloup and C. Guizard, *Nat. Mater.*, 2009, **8**, 966.
35. C. Korber, G. Rau, M. D. Cosman and E. G. Cravalho, *J. Cryst. Growth*, 1985, **72**, 649.
36. G. Gay and M. A. Azouni, *Cryst. Growth Des.*, 2002, **2**, 135.
37. N. O. Shanti, K. Araki and J. W. Halloran, *J. Am. Ceram. Soc.*, 2006, **89**, 2444.
38. A. M. Anderson and M. G. Worster, *Langmuir*, 2012, **28**, 16512.
39. R. W. Style, S. S. L. Peppin, A. C. F. Cocks and J. S. Wettlaufer, *Phys. Rev. E*, 2011, **84**, 1.
40. X. Wang, J. C. Yu, C. Ho, Y. Hou and X. Fu, *Langmuir*, 2005, **21**, 2552.
41. A. Kitada, G. Hasegawa, Y. Kobayashi, K. Kanamori, K. Nakanishi and H. Kageyama, *J. Am. Chem. Soc.*, 2012, **134**, 10894.
42. L. Liborio and G. Mallia, *Phys. Rev. B*, 2009, **79**, 245133.
43. V. Eyert, U. Schwingenschlögl and U. Eckern, *Chem. Phys. Lett.*, 2004, **390**, 151.
44. S. Siracusano, V. Baglio, C. D´Urso, V. Antonucci and A. S. Aricò, *Electrochim. Acta*, 2009, **54**, 6292.
45. U. Diebold, *Surf. Sci.Rep.*, 2003, **48**, 53.
46. K. Szot, M. Rogala,W. Speier, Z. Klusek, A. Besmehn and R. Waser, *Nanotechnology*, 2011, **22**, 254001.
47. M. E. Mycielska and M. B. Djamgoz, *J. Cell. Sci.*, 2004, **117**, 1631.
48. M. S. Markov, *Electromagn. Biol. Med.*, 2007, **26**, 257.
49. W. A. Catterall, E. Perez-Reyes, T. P. Snutch and J. Striessnig, *Pharmacol. Rev.*, 2005, **57**, 411.
50. I. S. Kim, Y. M. Song, T. H. Cho, H. Pan, T. H. Lee, S. J. Kim and S. J. Hwang, *Tissue Eng, Part A*, 2011, **17**, 1327.
51. C. D. McCaig, A. M. Rajnicek, B. Song and M. Zhao, *Physiol. Rev.*, 2005, **85**, 943.
52. L. Li, Y. H. El-Hayek, B. Liu, Y. Chen, E. Gomez, X. Wu, K. Ning, N. Chang, L. Zhang, Z. Wang, X. Hu and Q. Wan, *Stem Cells*, 2008, **26**, 2193.
53. A. M. Rajnicek, S. Britland and C. D. McCaig, *J. Cell Sci.*, 1997, **110**, 2905.
54. A. M. Rajnicek and C. D. McCaig, *J. Cell Sci.*, 1997, **110**, 2915.
55. Z. Huang and X. Jiang, *J. Mater. Chem. C*, 2013, **1**, 7652.

Graphical Abstract for

2D-ice templated titanium oxide films as advanced conducting platforms for electrical stimulation

Hernán E. Romeo, Fernando Trabadelo, Matías Jobbágy and Rodrigo Parra

Controlling film surface properties (topography and chemistry) while executing electrical stimulation is one of the most addressed research topics in materials chemistry. In this work, titanium oxide conducting films were *2D*-structured by directional freezing and tested as advanced platforms for electrical stimulation.